4

Spectral Properties of Plasma from a Planar Water Microjet Irradiated at Normal Incidence

4.1 Plasma production by femtosecond laser pulses

In chapter one, when the interaction of laser with matter is discussed, the response of a single atom to an intense laser field is considered. However for solids and liquids, at the interaction region, the number of atoms exposed to the laser field becomes close to the solid density (10^{23} atoms/cm^3). Even though all the basic ionization mechanisms discussed in chapter one remain valid for the interaction of laser with solid density matter, due to the availability of a very large number of atoms, there will be several other interactions occurring between the electrons and ions. This collective medium of electrons and ions existing with charge quasineutrality is named as '*plasma*', which comprises 99% of the 'visible' matter in the universe (90% of the entire universe is nonradiative 'Dark Matter' that gravitates). The existence of a very small amount of charge separation over a very short spatial scale for a very short time interval is known as the quasineutrality of plasma [Krishan, V.]. The interaction of laser with plasma is theoretically described by considering a two fluid model, whereas a numerical description is based on the *particle in a cell* simulation. The formation of plasma under an intense laser field can be understood as the ionization of the atoms in the focal volume by any of the optical ionization mechanisms described previously, when the input laser intensity is sufficiently high. For a femtosecond laser pulse the dominant ionization mechanisms will be tunnel ionization and above the barrier ionization. The electrons freed in this way are further accelerated in the laser field. In a solid density material, the electrons accelerated by the quiver motion will collide with the nearby neutral atoms inducing collisional ionization,

unlike the less dense atomic systems where the quiver motion is uninterrupted. Thus along with optical ionization, collisional ionization also is present in solid density materials in the femtosecond laser excitation regime. The plasma is formed by the leading edge of the laser pulse itself, and the electrons collectively respond to the trailing edge of the coherent laser pulse, creating plasma waves and several other interesting responses to the electric and magnetic fields of the pulse. There are different mechanisms by which the plasma absorbs the laser pulse, thereby increasing its temperature leading to the emission of extremely energetic photons, electrons and ions.

In solid density plasma, the electron-ion collision time will be less than the duration of the laser (femtosecond) pulse. Hence the time duration of the laser pulse determines the time scales of the temperature changes in the plasma. The expansion of such solid-density plasma occurs on a still longer timescale. Plasma expansion will remove the density discontinuity at the solid surface so that the laser pulse can see a gradient in the plasma density. On the other hand for short laser pulses the plasma is not expanded much, so that the laser pulse sees a steep gradient in the plasma density. Thus under the short pulse interaction, the laser pulse essentially interacts with a still-solid target. The density is high so that the electron mean free path decreases. From such interactions a short burst of continuum radiation as well as discrete emission lines can be observed. The charge state of the ions is determined by the peak intensity of the laser pulse, the plasma density determined by the atomic density of the material, and the physical dimensions of the plasma determined by the intensity distribution of the incident laser pulse. The random re-collisions of free electrons with the ions give a continuous emission spectrum, known as the ‘Bremsstrahlung emission’, of which the emission spectral intensity falls exponentially with increase in photon frequency.

4.1.1 Plasma: Some basic properties

In a plasma, the motion of every charge is determined by the collective system of charges, as all the charges are influencing other charges, while being influenced by the other charges. As the different charges move in the plasma, there will be localized concentrations of positive and negative charges producing electric fields. However, this charge separation exists only in the microscopic scale. Origin of this charge separation is from thermal motions of the electrons and ions in the plasma. This net microscopic charge separation creates an electric field in that region such that the electrostatic energy per charge will not exceed the thermal energy of the particle. This will make the charge separation exist only for a short duration of time.

Debye length

Considering the microscopic short-duration charge separation in a plasma, the one dimensional electric field due to a net charge density Q existing over a region of spatial extent l is given by

$$E = Ql/\varepsilon_0 \qquad \text{(In SI units)} \tag{4.1}$$

and the electrostatic energy of an electron or a single positive charge like proton is given as $Qel^2/2\varepsilon_0$. The average thermal energy per particle with one degree of freedom is given as $k_B T/2$ (for electron $T \equiv T_e$). Hence under the condition of quasineutral charge separation,

$$\frac{Qel^2}{2\varepsilon_0} \le \frac{k_B T}{2}. \tag{4.2}$$

For a plasma with an electron density 'n_e' the charge density $Q = n_e e$. Hence the spatial scale of charge separation is given by

$$l \le \left(\frac{\varepsilon_0 k_B T_e}{n_e e^2} \right)^{1/2} \equiv \lambda_{De} \tag{4.3}$$

and this length of microscopic charge separation in a plasma is known as the *Debye length* of the electrons in a plasma, as the ions are considered to be nearly

stationary. This is the length at which the movements and collisions of individual charge particles have to be considered [Krishan, V.], [Kruer, W.L.]. This distance, also referred to as the *screening distance*, gives a spatial extent over which the collective behaviour of the plasma is to be considered. Higher the density, shorter will be the Debye length. Within this distance the individual charges are important, and beyond this distance, the effective time varying spontaneous electrostatic field created by the microscopic charge separation is important, in the behaviour of plasma. The number of particles in a sphere of radius λ_{De} (the Debye sphere) is given by

$$N_D = \frac{4}{3}\pi\lambda_{De}^3 \tag{4.4}$$

and in order to consider the system enclosed in a volume defined by the Debye length as a statistical system with a specified temperature and number density, it should contain a large number of particles. i.e., $N_D >> 1$.

Electron-plasma frequency

The time duration τ_e for which the microscopic charge separation can exist in a plasma is determined by the time taken by the electron with a mean thermal speed of V_e to travel the distance l between the electron and the ions:

$$V_e = \left(\frac{k_B T_e}{m_e}\right)^{1/2} \tag{4.4}$$

and

$$\tau_e = \frac{l}{V_e} = \left(\frac{\varepsilon_0 m_e}{n_e e^2}\right)^{1/2} \equiv \omega_{pe}^{-1} \tag{4.5}$$

where ω_{pe} is the electron *plasma frequency*, i.e., the frequency at which the microscopic electron separation from the ions oscillates or the microscopic charge density fluctuation oscillates. In other words it gives the frequency with which the microscopic electrostatic force set by the charge separation fluctuates. From equation 4.5 it can be seen that, larger the electron density in the plasma larger

will be the electron plasma frequency. In order to ensure that there is a finite spatial scale of charge separation, the electron mean free path, the distance traveled by an electron before it undergoes a collision, should be much larger than the Debye length. i.e, the electron plasma frequency should be much larger than the electron – ion collision frequency:

$$\omega_{pe} >> \gamma_{ei} \tag{4.6}$$

4.2 Plasma absorption mechanisms

When a laser beam passes through a plasma, the plasma absorbs light in different ways depending on the nature of the plasma and the laser pulse. Either the response of individual electrons or the response of collective oscillations in the plasma will form the underlying mechanism for energy absorption from the laser field. The kind of mechanism being evoked is usually determined by the pulse width, polarization, angle of incidence etc. of the incident laser field.

4.2.1 Collisional absorption

At relatively low intensity, the main energy transfer mechanism between the laser pulse and the plasma is collisional absorption or inverse Bremsstrahlung absorption [Kruer, 1988], [Batani, D.]. Collisional behaviour becomes important when the number of electrons in the Debye sphere is less. The electrons performing quiver oscillations in the laser field undergo collisions with the ions thereby converting a part of the coherent oscillation energy into thermal energy of the electrons and thus heating up the plasma.

In a plasma charged particles continuously feel the Coulomb force due to the other particles, and hence undergo a change in momentum after each of these interactions. The Coulomb collision between two charged particles can be treated as the motion of a single particle of a reduced mass and a relative velocity moving in the Coulomb force field. The particle feels the force for a time for which it is in the neighbourhood of the other particle. Hence the change in momentum will be the product of the electrostatic force experienced by the particle and the time of

interaction. For large angle deflection the change in momentum of a particle is of the order of its momentum. The collisions in the plasma lead to the equilibration of the energy of the colliding particles leading to thermalization with a resultant average temperature. During each collision, energy is transferred from the more energetic particle to the less energetic particle. In a fully-ionized plasma three types of collisions can happen: electron-electron collisions, ion-ion collisions and electron-ion collisions. After the large angle collisions between particles of identical masses, both the particles will have nearly equal energies. Hence for electron-electron and ion-ion collisions the inverse of their collision frequencies gives the time in which they reach an equilibrium temperature among the respective species. But for an electron-ion collision, only a fraction of the electron energy is transferred to the ion in each collision and hence thermal equilibration between electrons and ions will take more time than that between identical species. This means that electrons and ions in a plasma can remain at different temperatures for a longer time than the ion species and the electron species themselves can do. This leads to a common temperature among the ions and electrons separately. Thus a plasma can be characterized by two temperatures, with one temperature to the ions and one to the electrons [Krishan, V.].

The change in momentum experienced by an electron of mass m_e moving with a velocity ν during collision with an ion of charge Ze is given by multiplying the Coulomb force by the time of interaction ($2b/\nu$), with *b* being the impact parameter (the distance of closest approach). If the electron undergoes many such collisions with randomly spaced ions, there will be a net change in the mean square velocity of the electron. When the electron is scattered through a large angle as a result of the collision with the ion, the change in velocity of the electron will become as large as the velocity of the electron itself. The mean rate at which this large change in the mean electron velocity occurs is referred to as the *electron-ion collision frequency*. For a Maxwellian velocity distribution, this collision frequency is given as:

$$\gamma_{ei} = \frac{Z n_e e^4 \ln\Lambda}{3(2\pi)^{3/2} \varepsilon_0^2 m_e^{1/2} (k_B T_e)^{3/2}} \tag{4.7}$$

Λ being the ratio of the maximum (Debye length) to minimum (larger of the classical distance of closest approach or the De Broglie wavelength of electron) impact parameter. ln Λ is referred to as the Coulomb logarithm.

Given the collisional frequency of electron-ion collisions one can obtain the damping experienced by an electromagnetic wave passing through such a collisional plasma, which gives the amount of collisional absorption suffered by the laser pulse. Considering the motion of the electron in the laser electric field and incorporating the damping due to electron-ion collision, the dielectric function of the collisional plasma, for the light frequency ω, can be obtained as:

$$\varepsilon = 1 - \frac{\omega_{pe}^2}{\omega^2 \left(1 + i\frac{\gamma_{ei}}{\omega}\right)} \tag{4.8}$$

The dispersion relation for light wave in a collisional plasma can be derived as:

$$\omega^2 = k^2 c^2 + \frac{\omega_{pe}^2}{\left(1 + i\frac{\gamma_{ei}}{\omega}\right)} \tag{4.9}$$

where the imaginary frequency component indicates collisional damping of the light wave in the plasma.

The efficiency of collisional absorption decreases with decrease in the laser pulse width. As the laser pulse intensity becomes greater than 10^{15} W/cm^2, the electron temperature increases significantly [Rozmus *et al.*], because the rate at which the electrons gain energy is much larger than the rate at which the electrons thermalize with other electrons [Pert, G.J.]. At very high laser intensities, the electron quiver energy will be so large that the quiver velocity dominates the thermal velocity of the electrons. Under this condition the collisional absorption is no longer a dominant laser absorption mechanism in plasma [Rae & Burnett]. For high density plasma, it is indicated that collisional

absorption, with nonlinear terms, is an efficient absorption mechanism [Kato e*t al.*].

4.2.2 Collisionless absorption

When the number of electrons in the Debye sphere is very large, collisional effects due to discrete particle encounters can be neglected. Under such a situation the laser absorption in the plasma can be attributed to collisionless process like resonance absorption. Collective behaviour of plasma becomes dominant here. Detailed treatment of the propagation of normal and obliquely incident *s* and *p* polarized light through a collisionless plasma is attempted in chapter 5, where Resonance Absorption is discussed.

Resonance Absorption is less effective if the plasma spatial density gradient is extremely sharp. This is because plasma waves can be set up only if there is a finite length of the plasma in existence. If the quiver amplitude of the electron in the laser field is greater than the plasma length, no plasma wave can be set up as the electron is taken farther away to the vacuum, breaking the plasma wave in each half cycle of the laser oscillation. Under this condition, another mechanism named 'vacuum heating' has to be considered. In this the electrons are dragged into the vacuum and sent back to the target with a velocity equal to the electron quiver velocity. A large number of electrons get accelerated to the target and their kinetic energy is deposited at the over- dense plasma where the laser field cannot penetrate [Brunel, F.]. The ratio of the absorbed power to the incident laser power per cycle in vacuum heating is given as:

$$f_{VH} = \left(\frac{\eta}{2\pi}\right)\left(\frac{e}{m\omega c\cos\theta}\right)\left(\frac{E_0^3}{E_L^2}\right) \tag{4.10}$$

where $\eta = 1.75\left(1 + 2\nu_{th}/\nu_{osc}\right)$. E_L is the incident laser field and E_0 is the total incident and reflected field [Brunel, F.], [Grimes *et al.*]. In vacuum heating the energy from the laser is directly coupled to the electrons.

Both RA and VH need obliquely incident p-polarized light as the excitation beam [Grimes *et al.*]. Hence the use of normally incident *p*-polarized light discussed in this chapter will not evoke these two mechanisms of plasma absorption. Other absorption mechanisms like Anomalous Skin effect (Important for $I \leq 10^{17}$ W/cm^2 ; laser pulse width should be less than 40fs and laser wavelength should be equal to 1 μm, as deduced from the basic conditions), Sheath inverse bremsstrahlung (laser wavelength should be less than or equal to 0.5μm)[Andreev et al.,] or sheath transit absorption (for *p*-polarized light obliquely incident on a steep plasma density gradient) are also not relevant under the present laser parameters and excitation conditions. Inverse Bremsstrahlung absorption is the only possible mechanism leading to plasma absorption under the normal laser incidence condition.

4.3 Incoherent white light emission

Laser produced plasma can be approximated as a blackbody at a particular temperature emitting incoherent radiation. The emission from a plasma can result from bound-bound transitions, free-bound transitions or free-free transitions, depending on the nature of the initial and final states of the electrons. The bound-bound transitions arising from neutral atoms in the excited state give rise to characteristic line emission. The free-bound transitions lead to recombination lines, where a free electron is captured by an ion to a bound state, resulting in a continuum with a minimum energy cut off indicating the ionization energy of the bound level [Griem, H. R.]. Free-free transitions give continuum emission referred to as Bremsstrahlung emission. If the frequencies emitted from a laser-produced plasma are in the visible region, the spectrum can be called incoherent white light from the plasma. This visible emission can occur if the plasma is heated only to emit in that region, or it can be the afterglow of a higher-energy plasma that emits in the higher frequencies too.

4.4 Femtosecond laser pulse interaction with a transparent dielectric

When a femtosecond laser pulse interacts with a transparent dielectric, plasma is created on the material surface. This plasma will reflect a major part of the laser pulse from the plasma critical electron density layer, allowing only the leading edge of the pulse to pass through. The absorbed energy is deposited at a very thin surface layer, thus creating a large energy density in the plasma [Feit *et al.*], [Stuart *et al.*]. The discussion here is mainly focused on water, though it is applicable for any dielectric with a wide band-gap. Water can be treated as an amorphous semiconductor with quasi-free states, in which the electrons have sufficient kinetic energy to move through the liquid without being trapped by localized potential wells. Hence it can be considered to have effective conduction and valence bands with a band-gap of 6.5eV [Williams, F.], [Kennedy, P. K.]. The evolution of free electron density acts as the center of the emission processes from the plasma. Since electron-phonon inelastic scattering occurs in the picoseconds time scale, under femtosecond excitation, energy transfer between electrons and ions can be neglected. The ionization process can be described by considering a rate equation for the free electron density given by

$$\frac{dn}{dt} = \alpha(I,n) + P(I) - \beta n^2 \tag{4.11}$$

where the first term indicates the change in electron density due to impact ionization, where an already free electron with sufficient kinetic energy leads to the production of new free electrons by collision. The second term represents the direct ionization of atoms by the laser pulse. Depending on the intensity of the input laser pulse, this can be multiphoton ionization, tunnel ionization or above the barrier ionization. This term is a function of only the input laser intensity. The third term represents the loss of free electrons due to recombination with ions. Since we consider femtosecond laser pulses there will not be any loss of electrons due to diffusion from the focal volume during the pulse [Feit *et al.*]. The impact ionization rate is given as:

$$\alpha(I,n) = 2\frac{\omega}{c}\frac{\mathrm{Im}\left(\sqrt{\varepsilon(n)}\right)I}{\left(\langle e_e\rangle + U\right)} \tag{4.12}$$

where ω is the laser frequency, c the velocity of light in free space, $\langle e_e \rangle$ the average free electron energy, U the band-gap energy and ε(n) the dielectric function. P(I) can be obtained from the Keldysh formulae [Keldysh, L.V.]. Studies on the penetration depth of the laser pulse show that most of the pulse energy is deposited within a surface layer of 20-30μm [Feit *et al.*]. Thus the plasma is formed at the surface and when it becomes dense, the laser pulse mostly gets reflected from the plasma. Hence, only the leading edge of the pulse will be transmitted through the medium since the latter part of the pulse will be reflected from the plasma.

4.5 Spectral blueshift

Laser light that is being scattered from a plasma with a rapidly varying refractive index shows a spectral blueshift. In the optical ionization of gases this has been reported at an intensity level of 10^{16} W/cm^2 [Wood *et al.,* 1991], [Penetrante *et al.*]. Spectral blue shift has also been reported for cluster plasma [Kim *et al.*] and for plasma from methanol microdroplets [Anand *et al.*]. When the ionization of a medium happens due to intense laser fields, the refractive index seen by the laser pulse suddenly changes from the refractive index of neutral atoms to that of the free electrons in the plasma. The optical polarizability (distortion in the charge distribution in an external electric field) of free electrons is much larger than the polarizability of neutral atoms and it is of the opposite sign. The rapid creation of plasma leads to a fast decrease in the refractive index of the medium. Due to this sudden change of refractive index, the laser pulse is phase-shifted to higher frequencies [Yablonovitch, E., 1988]. The frequency shift is given as:

$$\Delta\omega = -\frac{\omega_0}{c}\int_0^L \frac{\partial n_{RF}(x,t)}{\partial t}dx \tag{4.13}$$

where ω_0 is the original laser frequency, L the interaction length, and $n_{RF}(x,t)$ the index of refraction along the propagation direction. For an incident wavelength λ_0 and an interaction length L in the plasma, the shift in the wavelength is given by:

$$\Delta\lambda = -\frac{e^2 L\lambda_0^3}{2\pi m_e c^3}\frac{dn_e}{dt} \quad \text{(in cgs)} \tag{4.14}$$

where $\frac{dn_e}{dt}$ is the rate of change of free electron density [Wood *et al.* 1988], [Penetrante *et al.*].

4.6 Experimental results and discussion

Laser induced break down in aqueous media has been reported in literature for different pulse durations and frequencies [Feng *et al.*], [Vogel *et al.*], [Nahen & Vogel],[Kennedy et al.], [Noak & Vogel]. It is known that with nanosecond laser excitation, laser induced explosion of water microdroplets gives rise to characteristic hydrogen atom emissions superposed over a white light continuum [Eickmans *et al.*]. However, the presence of these characteristic lines has not been reported in the case of femtosecond laser pulse excitation before. In an earlier report, even visible radiation was not detected from aqueous plasmas for pulses shorter than 6ps, since the low blackbody temperature shifted the emission peak into the infrared. Likewise, femtosecond illumination of pure water in a cell had given only a spectroscopically featureless continuum, caused due to self phase modulation (SPM) [Kennedy *et al.*, 1997]. For water microdroplets, though femtosecond excitation produced a highly confined plasma and blackbody emission in the visible, characteristic line emission was not reported [Favre *et al.*].

In contrast to these reports, however, we were able to observe the characteristic H_α and H_β lines superposed over a visible continuum emission, when a thin planar water microjet of 250 μm thickness was excited with 100 femtosecond laser pulses. A prominent spectral blueshift is also observed at higher incident laser intensity. The pump intensities used are of the same order

(~10^{15}W/cm^2) as that was obtained within water microdroplets in an earlier work [Favre *et al.*]. Unlike in the water microdroplets no morphological increase of intensity will occur in the planar water microjet because it is thin, and also because self-focusing gets limited at these high intensities [Kennedy, P. K.]. The laser interaction with the water jet in the present studies is in the intensity regime of tunnel ionization. Plasma created at the surface and the interaction of the trailing part of the pulse with the thus created plasma determines the depth of penetration of the laser light into the medium.

The experiments are done with a mode-locked chirped pulse amplifier (CPA) Ti: Sapphire laser (Spectra physics TSA-10), delivering linearly polarized 100fs pulses at 810nm at a repetition rate of 10Hz. The beam is focused with a plano-convex lens (f = 20cm) and the jet containing circulating singly distilled water is placed at the focus. In a darkened room, white light emission could be seen with naked eyes at a relatively lower laser pulse intensity of 4.8x10^{14} W/cm^2. Spectra are recorded upto a maximum input laser intensity of 3.9x10^{15}W/cm^2. Input laser intensities are increased in steps of ~1.3x. The emission spectra are recorded using an Avantes fiber-optic spectrometer (AvaSpec-2048, set to 330-1100nm range with a resolution of 1.4nm). The collection lens, attached to the tip of the collection fiber of 600μm diameter, is placed at a distance of 10cm from the jet. The *p*-polarized laser light is incident normal to the water jet. Either a band-cut filter (for the laser wavelength) or a crossed polarizer is used to minimize the amount of scattered laser radiation reaching the collection fiber. For all the input laser intensities used, it is confirmed that no visible emission is produced from air, by recording the spectra with the water jet switched off. Figure 4.1 gives the emission spectra detected at the representative angle 115^0 to the laser beam direction. For other directions also the nature of the spectra remains the same, with changes in the spectral intensities for different angles of detection. As the input laser intensity is increased beyond 1.4x10^{15} W/cm^2, a peak is found to emerge at 656nm. This is the H_α line. At still higher laser intensities a peak

appears beyond 675nm. This originates from the prominent spectral blueshift of the scattered laser pulse which happens at higher laser intensities.

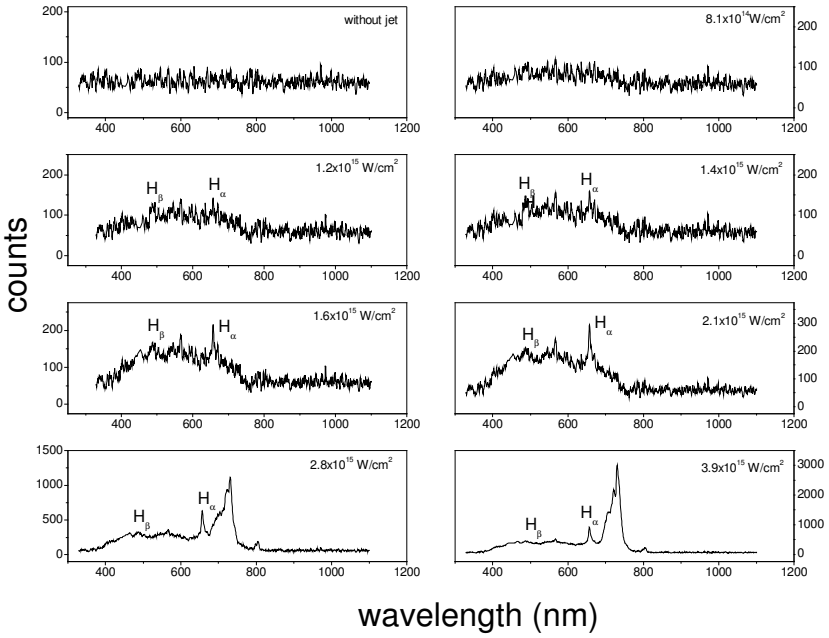

Fig. 4.1: Emission Spectra from singly distilled water excited at different intensities, observed at an angle of 115^0 to the laser beam direction, at 810nm, using 100fs laser pulses. A band-cut filter is used to attenuate radiation at and near the laser wavelength. H_α line can be seen prominently. Part of the blue shifted spectrum is seen at higher intensities of excitation.

In figure 4.2 spectra obtained with a crossed polarizer placed in front of the detector are given. By using the crossed polarizer instead of the band-cut filter, it is possible to record the wavelengths very close to the laser frequency also. It is seen that the spectrum falls completely on the anti-stokes side of the excitation wavelength.

Figure 4.3 shows the spectral blueshift on an expanded scale. It is observed that as the input pulse intensity is increased, the spectral peak blueshifts in general. Above $1.4x10^{15}$ W/cm^2 a shoulder appears on the blue side. Previous

studies in gases explain the broad blue shifted shoulder as from strong field ionization whereas the less blue shifted peak corresponds to collisional ionization [Wood *et al*., 1991]. In our experiment also, the increase in the input laser intensity increases the tunnel ionization and thus gives broader blue shifted shoulder as observed.

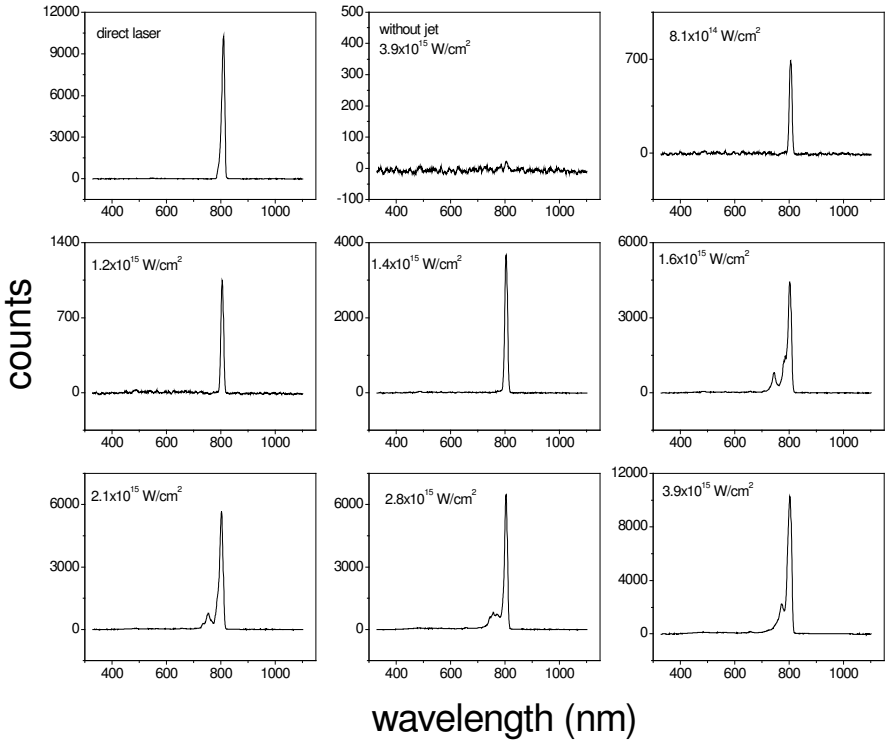

Figure 4.2: Emission Spectra from singly distilled water excited at different intensities, observed at an angle of 115^0 to the laser beam direction. In order to record the wavelengths near the laser frequency a polarizer is used in the crossed position (instead of the band-cut filter) to reduce the scattered laser intensity below the saturation level of the CCD. Spectral blueshift is seen. No emission is seen for wavelengths higher than the excitation wavelength.

Figure 4.4 gives the fit of equation (4.14) to the spectral blue shift shown in figure 4.3 for different input laser intensities. The quantity $L\frac{dn_e}{dt}$ is taken as

the fit parameter. From figure 4.4 it is observed that the product $L\frac{dn_e}{dt}$ remains the same ($1x10^{27}cm^{-2}s^{-1}$) without much change even when the input intensity is increased. At higher laser intensities the ionization rate will be higher, and the quantity $\frac{dn_e}{dt}$ will increase. The constancy of the product term $L\frac{dn_e}{dt}$ therefore implies that the propagation length L of the laser light in the plasma is reduced as $\frac{dn_e}{dt}$ or the laser intensity increases. This indicates that the plasma critical density is attained at shorter distances as the laser intensity is increased so that the latter

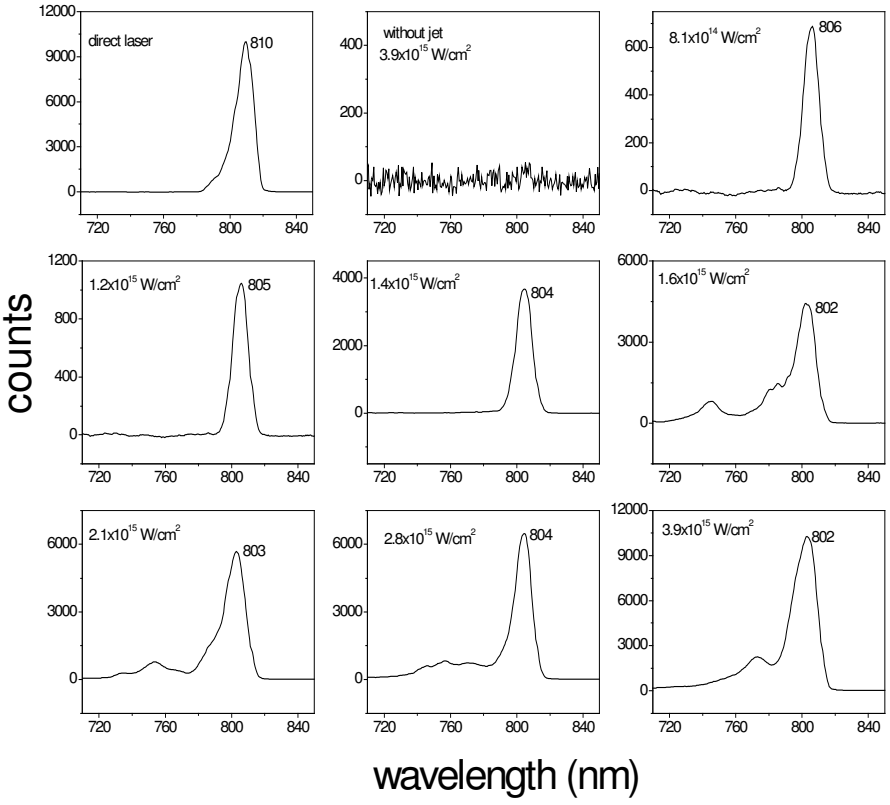

Figure 4.3: Spectral blueshift shown on an expanded scale. The blueshift generally increases with the intensity of the incident laser.

part of the laser pulse will be traversing only a shorter distance in the plasma before reaching the critical density region.

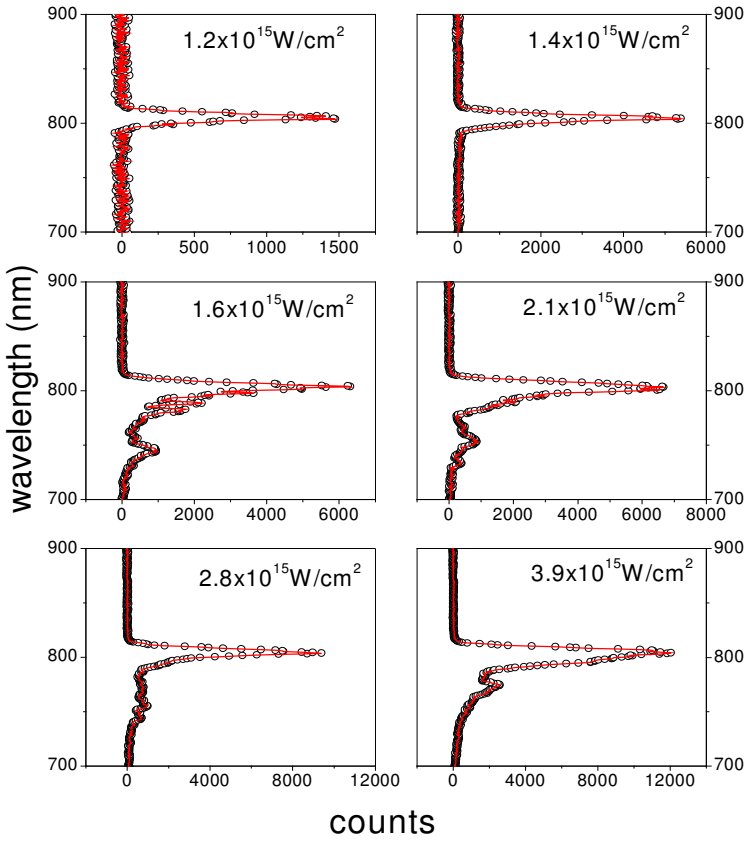

Figure: 4.4 Spectral blueshift. The solid lines are the fits to the experimental data using eqn.(4.14).

Figure 4.5 (a) shows the emission at an input laser intensity of 3.9×10^{15} W/cm^2 in an enlarged graph. In addition to the H_α line, a rather weak H_β line at 486nm and singly ionized oxygen line (OII) at 464nm, are also observed. Singly ionized nitrogen line is observed at 567nm. These characteristic lines are the result of electron recombination with the respective ions. The NII line is from the ionization of the air molecules present in the ambience. The first ionization energy of nitrogen is 14.6eV, which is comparable to the ionization energy of the

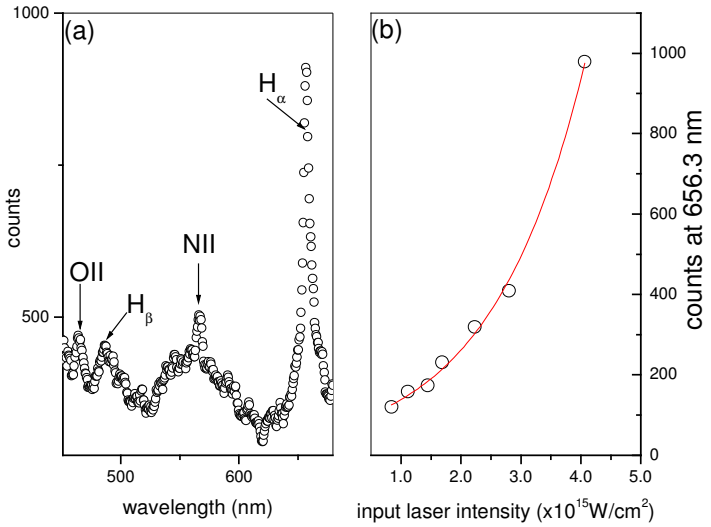

Fig.4.5: (a) Emission lines identified for an input laser intensity of 3.9×10^{15} W/cm^2. The emission is weaker for lower input laser intensities. OII (singly ionized oxygen line at 464nm), H_β line at 486.1 nm, NII (singly ionized nitrogen line at 566.6 nm) and H_α line at 656.3nm can be seen. (b) Growth of the H_α line (656.3 nm) with increasing laser intensity. The solid curve is an exponential fit. The *e-folding intensity* (the intensity interval in which the recombination line strength becomes e-times, i.e., 2.7 times, its previous value) is found to be 1.6×10^{15} W/cm^2 from the fit.

hydrogen atom and the first ionization energy of oxygen atom. Figure 4.5(b) shows that H_α line intensity grows exponentially with the input laser intensity. Since this is a recombination line, the exponential growth implies that the ionization also grows exponentially with the input intensity. As the ionization happens during the pulse lifetime, the rate of formation of the free electrons grows exponentially with input intensity. This is in agreement with the observations from the spectral blue shift, where it is considered that the rate of change of free electron density increases with increase in the input laser intensity.

We did a spectrally resolved polarization analysis of the plasma emission, and the results are shown in figure 4.6. Emissions in the 350 - 640nm region (continuum), as well as that of the 640 – 675nm region (containing the H_α line) are found to be unpolarized. However, the broad emission observed in the 675 – 730nm region is polarized in the plane of the pump pulse. This spectral region is the result of spectral blueshift.

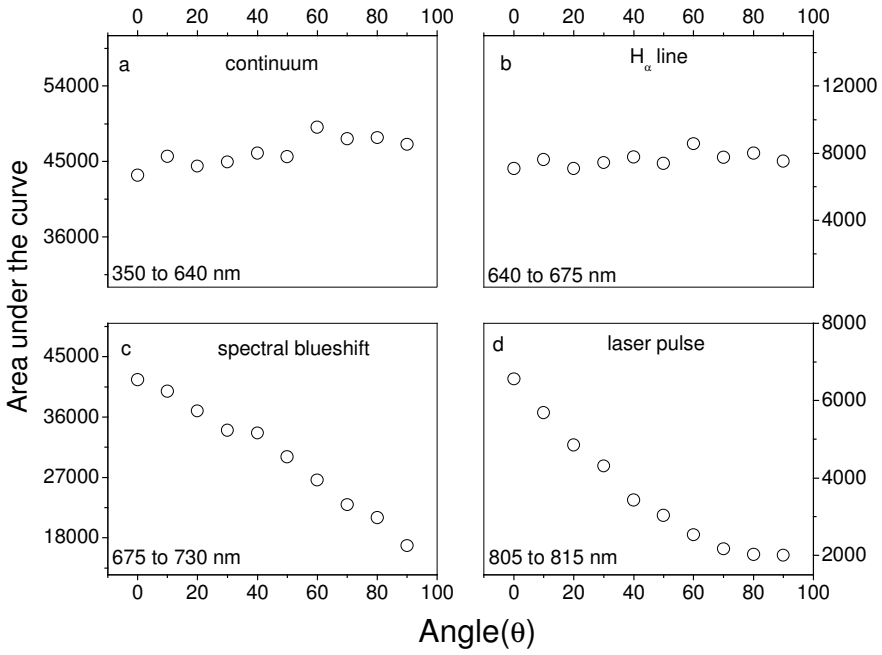

Fig.4.6: Polarization of emitted radiation in different spectral bands. The input laser intensity is 3.9×10^{15} W/cm^2. The input laser polarization plane is taken as reference ($\theta = 0$). The regions of (a) continuum (350 to 640 nm), (b) H_α line (640 to 675 nm), and (c) spectral blueshift (675 to 730 nm) are shown. (d) polarization of the reflected laser pulse.

The absence of stokes frequencies confirms that plasma contributes substantially to the white light continuum emitted from the water jet. At the laser intensity levels considered here the leading edge of the pulse itself will be strong enough to ionize water. The trailing edge of the pulse sees the changing refractive index of the plasma and hence undergoes spectral blueshift to anti-stokes

frequencies. The absence of stokes lines shows that there are no sufficient neutral molecules to contribute to stokes frequencies.

The relative strength of the different bonds in water is as follows: Hydrogen bond (0.2eV) <covalent bond (3.6eV) < s orbital of Hydrogen atom (13.6eV) < 2s & 2p-orbitals of oxygen < 1s orbital of oxygen atom. Ionization of water is essentially the breaking of these different bonds. From the emission spectra we can infer the nature of bond breaking to some extent under the present excitation scheme. Hydrogen bonding in water dynamically ruptures even under ordinary conditions due to the low bond energy. The recombination lines indicate that H^+ ions are present in the plasma. The observed spectra can be attributed to the breaking of the covalent bonds in water followed by the ionization of the hydrogen atom. The first ionization energy of oxygen is 13.6eV (energy required to remove the outermost electron from a neutral atom), which is comparable to the ionization energy of the hydrogen atom. The second ionization energy of oxygen is 35.2eV. Single ionization of oxygen is possible under the present excitation scheme since the first ionization energy for oxygen atom is comparable to that of hydrogen atom. A relatively weak emission line is observed at 464nm corresponding to singly ionized oxygen (OII), which is shown in figure 4.5(a). No OIII line is seen at 500.7nm, which indicates that under the present laser produced ionization, only that ionization which requires an energy < 35.2eV happens. The optical field ionization of the atomic hydrogen and oxygen formed from the rupture of the covalent bond happens by tunnel ionization at the given laser intensity level. Electrons oscillating in the laser field will attain quiver energy, and when they pass through the potential of the ions they are captured leading to free-bound transitions with a continuum emission and a recombination line cut off. The H_α and H_β lines originate from the recombination of free electrons with hydrogen ions to form hydrogen atoms. As the input intensity is increased, more and more molecules get ionized to H^+ and O^+ and hence the dynamic free electron density becomes higher. This high free electron density that varies rapidly, strengthens the spectral blueshift of the trailing part of the laser pulse. From figure 4.5(b) it is

clear that the strength of the H_α line increases exponentially with a threshold of growth around 1.0×10^{15} W/cm^2. From figures 4.1 and 4.2 it can be seen that the spectral blueshift becomes prominent around the intensity of 1.6×10^{15} W/cm^2. This indicates that around and above 10^{15} W/cm^2 the rate of change of free electron density is large enough to cause an observable shift in the laser frequency. Since the spectra are recorded in the backward direction with respect to the laser direction, no other propagation broadening can be attributed to the spectral shift. This blueshift has its origin completely from the plasma dynamics.

To summarize, our experiments have shown that the excitation of a planar water jet with femtosecond laser pulses focused to an intensity of 10^{14} to 10^{15} W/cm^2 leads to the collisional ionization of water molecules, initialized by tunnel ionization, and the formation of plasma. For normal incidence of the p-polarized laser pulses, the plasma is heated by the inverse Bremsstrahlung absorption mechanism, as no plasma wave is excited under the normal incidence geometry. The emission from the plasma is identified as the incoherent emission from free-bound recombination transitions and a spectral blueshift of the scattered laser pulse.